

# i-process nucleosynthesis: observational evidences from CEMP stars

Partha Pratim Goswami<sup>1</sup>, Aruna Goswami<sup>1</sup>

<sup>1</sup>Indian Institute of Astrophysics, Koramangala, Bangalore 560034, India.

\*Corresponding author. E-mail: partha.pg@iiap.res.in; aruna@iiap.res.in

MS received 30 August 2020; accepted 05 October 2020

**Abstract.** The surface chemical compositions of a large fraction of Carbon-Enhanced Metal-Poor (CEMP) stars, the so-called CEMP-r/s stars, are known to exhibit enhancement of both s- and r-process elements. For these stars, the heavy element abundances cannot be explained either by s-process or r-process nucleosynthesis alone, as the production sites of s- and r-process elements are very different, and these two processes produce distinct abundance patterns. Thus, the observational evidence of the double enhancement seen in CEMP-r/s stars remains a puzzle as far as the origin of the elements is concerned. In this work, we have critically analysed the observed abundances of heavy elements in a sample of eight CEMP-r/s stars from literature, to trace the origin of the observed double enhancement. Towards this, we have conducted a parametric-model based analysis to delineate the contributions of s- and r-process nucleosynthesis to the observed elemental abundances. We have further examined if the i-process (intermediate process) nucleosynthesis, that occurs at a high neutron-density ( $n \sim 10^{15} \text{ cm}^{-3}$ ) produced during proton-ingestion from a H-rich envelope to the intershell region of an AGB star, that is capable of producing both r- and s-process elements in a single stellar site, could explain the observed abundance patterns of the sample stars. Our analysis shows that the observed abundance patterns of the selected sample of CEMP-r/s stars could be fairly well reproduced using the i-process model yields.

**Keywords.** Stars—Nucleosynthesis—i-process.

## 1. Introduction

Most of the elements heavier than iron are produced by slow ('s') and rapid ('r') neutron-capture nucleosynthesis processes. In the slow-neutron capture process (s-process) the timescale for neutron-capture is usually much longer than that for the  $\beta$ -decay of unstable nuclei along the s-process path, whereas, in the rapid neutron-capture process (r-process) the timescale for neutron-capture is much shorter than the  $\beta$ -decay process. While the s-process operates with a neutron-density of  $10^6\text{--}10^8 \text{ cm}^{-3}$  (Busso *et al.* 1999) in the inter-pulse phases of low and intermediate-mass AGB stars (Gallino *et al.* 1998), the r-process requires very high temperatures and neutron fluxes ( $n > 10^{20} \text{ cm}^{-3}$ ) and is expected to occur during supernova explosions and neutron star mergers (Thielemann *et al.* 2011; Wehmeyer *et al.* 2015). These two processes are characterized by distinct elemental abundance patterns. The surface chemical compositions of a large fraction of Carbon-Enhanced Metal-Poor (CEMP) stars are known to exhibit enhancement of s-process elements (CEMP-s stars), a few exhibit enhancement in r-process elements (CEMP-r stars), a sizeable fraction shows en-

hancement of both s- and r-process elements (CEMP-r/s stars) and a few stars do not show enhancement of heavy elements (CEMP-no stars) (Beers & Christlieb 2005; Aoki *et al.* 2007). In general, CEMP stars are characterized by  $[\text{Fe}/\text{H}]^1 < -1.0$  and  $[\text{C}/\text{Fe}] > 1.0$  and Barium and Europium are considered as the representative elements of s- and r-process respectively (Beers & Christlieb 2005). Chemical composition studies on (CEMP)-r/s stars have revealed that the observed heavy element abundances cannot be explained either by s-process or r-process nucleosynthesis alone (Aoki *et al.* 2015, 2017). In order to explain the abundance pattern of the CEMP-r/s stars different formation scenarios have been proposed, involving different production sites for the s- and r-process elements (Jonsell *et al.* 2006; Lugaro *et al.* 2009; Abate *et al.* 2016). All these scenarios are, however not free from certain uncertainties, either in explaining the observed frequency of these stars, or the observed abundance patterns. An alternative process called 'i-process (intermediate process) nucleosynthesis' has recently been suggested as

<sup>1</sup>**Notation:**  $[A/B] = \log(N_A/N_B)_* - \log(N_A/N_B)_\odot$ , where  $N_A$  and  $N_B$  are number densities of elements A and B respectively.

a possible production mechanism for CEMP-r/s stars (Dardelet *et al.* 2014; Hampel *et al.* 2016; Hampel *et al.* 2019). Although it has been known for long (Cowan & Rose, 1977) that the proton-ingestion from the convective envelope to the intershell region of AGB stars can produce high neutron flux which can initiate i-process nucleosynthesis, only very recently it has been explored to understand the observed abundance patterns of CEMP-r/s stars on the basis of i-process (Dardelet *et al.* 2014; Hampel *et al.* 2016; Hampel *et al.* 2019). Different sites have been proposed for the proton-ingestion episodes (PIE), such as core-helium flash (Fujimoto *et al.* 1990; Lugaro *et al.* 2009), the most massive AGB stars (Jones *et al.* 2016), the super AGB stars (Doherty *et al.* 2015). However, the physical conditions under which proton-ingestion can take place still remain a matter of debate. Many details regarding the site of the i-process nucleosynthesis that operates with neutron densities,  $n \sim 10^{15} \text{ cm}^{-3}$  also remain poorly understood.

In this work, in order to understand the origin of the abundance patterns of heavy elements in CEMP-r/s stars, we have chosen a sample of eight stars reported to be CEMP-r/s stars by various authors (Goswami *et al.* 2006; Goswami & Aoki 2010; Allen *et al.* 2012; Hansen *et al.* 2019; Purandardas *et al.* 2019) based on their estimates of abundances and abundance ratios of heavy elements for these stars. We have performed a parametric-model based study to delineate the contributions of s- and r-process to the observed heavy element abundances. With reference to the sample stars, we have discussed and examined different formation scenarios to understand the processes responsible for the double enhancement seen in these stars. We find, that using i-process model yields we could reproduce the observed abundance patterns of heavy elements of the sample of CEMP-r/s stars under this study.

In Section 2., we have discussed in brief, the sample of CEMP-r/s stars taken from the literature for this study. Section 3. discusses the procedure and results of the parametric-model based study. In Section 4.1, different formation scenarios have been discussed in the context of the abundance pattern observed in the sample stars. Section 4.2 discusses the i-process models and results of the comparison of the model predictions with the observed heavy-element abundances of our sample stars. We have drawn the conclusions in Section 5.

**Table 1. Atmospheric parameters of the sample stars.**

Star name	$T_{eff}$ (K)	log g	$\zeta$ ( $\text{km s}^{-1}$ )	[Fe/H]
CD-28 1082 <sup>1</sup>	5200	1.90	1.42	-2.45
CS 29503-010 <sup>2</sup>	6050	3.66	1.60	-1.70
CS 29528-028 <sup>2</sup>	7100	4.27	1.20	-2.15
HD 209621 <sup>3</sup>	4500	2.00	2.00	-1.93
HE 0002-1037 <sup>4</sup>	5010	2.00	1.80	-2.40
HE 0059-6540 <sup>4</sup>	5040	2.10	1.80	-2.20
HE 0151-6007 <sup>4</sup>	4350	1.00	2.10	-2.70
HE 1305+0007 <sup>5</sup>	4750	2.00	2.00	-2.01

1. Purandardas *et al.* (2019), 2. Allen *et al.* (2012), 3. Goswami & Aoki (2010), 4. Hansen *et al.* (2019), 5. Goswami *et al.* (2006).

## 2. Sample of CEMP-r/s stars: CD-28 1082, CS 29503-010, CS 29528-028, HD 209621, HE 0002-1037, HE 0059-6540, HE 0151-6007, HE 1305+0007

The objects are selected following CEMP stars criteria (i.e.,  $[\text{Fe}/\text{H}] < -1$ , and  $[\text{C}/\text{Fe}] > 0.7$ ). In our sample, the CEMP-r/s stars have metallicity in the range  $-1.70 < [\text{Fe}/\text{H}] < -2.70$ . In Purandardas *et al.* (2019) we have derived the atmospheric parameters and, for the first time, estimated the elemental abundances of CD-28 1082. The object was found to be a CEMP-r/s star with  $[\text{Ba}/\text{Fe}] = 2.09$ ,  $[\text{Eu}/\text{Fe}] = 2.07$  and  $[\text{Ba}/\text{Eu}] = 0.02$  with a  $^{12}\text{C}/^{13}\text{C}$  ratio  $\sim 16$ . The objects HE 0002-1037, HE 0059-6540 and HE 0151-6007 have been reported to be CEMP-r/s by Hansen *et al.* (2019). These three objects exhibit abundances of Ba and Eu in the ranges  $1.7 < [\text{Ba}/\text{Fe}] < 2.3$  and  $1.5 < [\text{Eu}/\text{Fe}] < 2.3$  with  $[\text{Ba}/\text{Eu}] < 0.5$  in each case. Hansen *et al.* (2019) estimated the  $^{12}\text{C}/^{13}\text{C}$  ratio to be 24 and 1 for the objects HE 0002-1037 and HE 0059-6540 respectively. The kinematic analysis shows that all these four sample stars belong to the inner halo population in the Galaxy. Allen *et al.* (2012) classified the objects CS 29503-010 and CS 29528-028 to be CEMP-r/s stars with  $[\text{Ba}/\text{Fe}] = 1.81$  &  $2.49$  and  $[\text{Eu}/\text{Fe}] = 1.69$  &  $2.16$  respectively on the basis of their analysis. Elemental abundances of two CEMP-r/s stars HE 1305+0007 and HD 209621 have been taken from Goswami *et al.* (2006) and Goswami & Aoki (2010) respectively. Tsuji *et al.* (1991) and Goswami *et al.* (2006) estimated  $^{12}\text{C}/^{13}\text{C}$  ratio to be  $\sim 10$  for both the objects HD 209621 and HE 1305+0007.

The atmospheric parameters of the sample stars are presented in Table 1. The abundance ratios of neutron-capture elements and carbon with respect to Fe are presented in Table 2.

**Table 2. Abundance ratios of neutron-capture elements of the sample stars.**

Star name	[Fe/H]	[C/Fe]	[Sr/Fe]	[Y/Fe]	[Zr/Fe]	[Ba/Fe]	Ref
CD-28 1082	-2.45	2.19	1.44	1.61	-	2.09	1
CS 29503-010	-1.70	1.65	1.13	1.09	1.26	1.81	2
CS 29528-028	-2.15	2.76	1.72	1.99	2.17	2.49	2
HD 209621	-1.93	1.25	1.02	0.36	1.80	1.70	3
HE 0002-1037	-2.40	1.90	<1.00	0.40	-	2.00	4
HE 0059-6540	-2.20	1.40	1.20	0.40	-	1.70	4
HE 0151-6007	-2.70	1.70	1.10	0.80	-	2.30	4
HE 1305+0007	-2.01	1.84	0.86	0.73	2.09	2.32	5

Star name	[La/Fe]	[Ce/Fe]	[Pr/Fe]	[Nd/Fe]	[Sm/Fe]	[Eu/Fe]	Ref
CD-28 1082	1.55	1.97	2.30	1.99	2.29	2.07	1
CS 29503-010	2.16	2.05	-	2.31	2.34	1.69	2
CS 29528-028	2.21	2.47	-	2.54	-	2.16	2
HD 209621	2.41	2.04	2.16	1.87	1.46	1.35	3
HE 0002-1037	2.00	1.70	2.10	2.10	-	1.70	4
HE 0059-6540	1.60	1.40	1.40	1.70	-	1.50	4
HE 0151-6007	2.50	2.40	2.60	2.60	-	2.30	4
HE 1305+0007	2.56	2.53	2.38	2.59	2.60	1.97	5

References: 1. Purandardas *et al.* (2019), 2. Allen *et al.* (2012), 3. Goswami & Aoki (2010), 4. Hansen *et al.* (2019), 5. Goswami *et al.* (2006).

### 3. Parametric-model based study

In order to understand the origin of the observed abundances in the sample stars, it is important to identify the contribution of the dominant neutron-capture process. Following the procedure described in Goswami *et al.* (2010) and references therein, we have performed a parametric-model based study to trace the contributions of s- and r-process nucleosynthesis to the observed abundances of the heavy elements. We have normalized the Solar s- and r-process isotopic abundances of the stellar models of Arlandini *et al.* (1999) to the barium abundances of the corresponding CEMP-r/s stars. The observed elemental abundances of the sample stars are then fitted with the parametric model function  $\log \epsilon_i = C_s N_{is} + C_r N_{ir}$ , where  $N_{is}$  indicates the normalized abundance from s-process,  $N_{ir}$  indicates the normalized abundance from r-process.  $C_s$  indicates the component coefficient that corresponds to contributions from the s-process and  $C_r$  indicates the component coefficient that corresponds to contributions from the r-process.

The best fitting coefficients and  $\chi^2$  values are presented in Table 3. Figure 1 shows the best model fits with the observed abundances of the sample stars. Goswami & Aoki (2010) performed a parametric-model based analysis of the heavy element abundances observed in HD 209621 and HE 1305+0007 and concluded that similar contributions of both s- and r-process are required to explain the abundance pattern of the stars (see Figure 5 of Goswami & Aoki, 2010). WE have confirmed these results based on our analysis.

**Table 3. Best-fit coefficients and  $\chi^2$  for the parametric model function  $\log \epsilon_i = C_s N_{is} + C_r N_{ir}$**

Star name	$C_s$	$C_r$	$\chi^2$
CD-28 1082	0.48	0.52	4.97
CS 29503-010	0.37	0.63	6.76
CS 29528-028	0.48	0.52	1.06
HD 209621 <sup>a</sup>	0.57	0.52	1.80
HE 0002-1037	0.41	0.59	10.73
HE 0059-6540	0.47	0.53	7.83
HE 0151-6007	0.21	0.79	11.91
HE 1305+0007 <sup>a</sup>	0.47	0.53	1.07

<sup>a</sup>- Goswami & Aoki (2010).

### 4. Discussions

#### 4.1 Different formation scenarios of CEMP-r/s stars

In order to explain the peculiar abundance pattern of CEMP-r/s stars, different authors have proposed several formation scenarios (Jonsell *et al.* 2006; Lugaro *et al.* 2009; Abate *et al.* 2016). Here, we have discussed briefly some of the scenarios that are considered relevant for the sample of CEMP-r/s stars under this study.

(i) Radiative levitation, where the partially ionized heavy elements having large photon absorption cross-sections are pushed outwards by radiative pressure, could be a possible scenario for the observed overabundance of heavy elements in the CEMP-r/s stars. However, the simulations of Richard *et al.* (2002) and

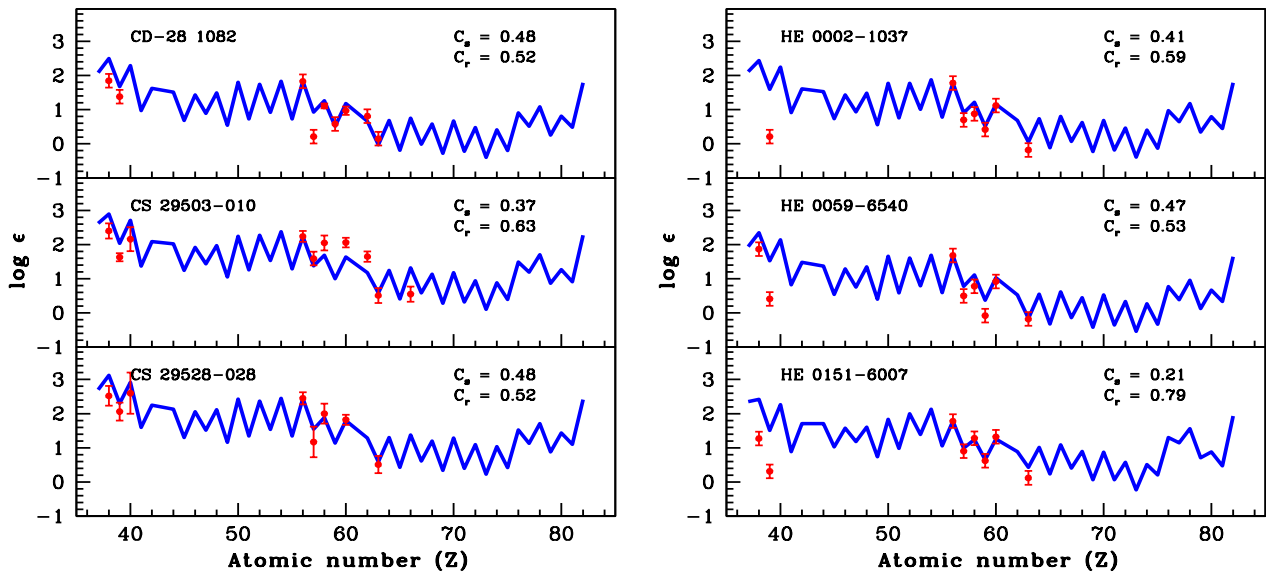


**Figure 1.** Solid curve represents the best fit for the parametric-model function  $\log \epsilon_i = C_s N_{is} + C_r N_{ir}$ , where  $N_{is}$  and  $N_{ir}$  represent the abundances due to s- and r-process respectively (isotopic abundances from the Stellar model of Arlandini *et al.* (1999) are normalized to the Ba abundances of the corresponding stars). The points with error bars indicate the observed abundances.

Matroziis & Stancliffe (2016) have shown that the process of radiative levitation can occur in the hot stars in their main-sequence and main-sequence turn-off phases of evolution due to their thin convective envelopes. The sample stars in this study are low-temperature objects with temperature in the range 4350 K – 7100 K, and the radiative levitation scenario may not be applicable to explain the observed abundance pattern of these stars. This scenario has also been discussed at length by Cohen *et al.* (2003), Jonsell *et al.* (2006) and Abate *et al.* (2016) and rejected as a possible formation mechanism of CEMP-r/s stars.

(ii) There are two scenarios where the enhancement of r-process elements in the CEMP-r/s stars is attributed to the r-process material enriched ISM from which the star is formed. In these scenarios, it is proposed that the enrichment of s-process elements is either due to self-contamination in its AGB phase (Hill *et al.* 2000; Cohen *et al.* 2003; Jonsell *et al.* 2006) or AGB pollution in a binary system (Hill *et al.* 2000; Cohen *et al.* 2003; Jonsell *et al.* 2006; Ivans *et al.* 2005; Bisterzo *et al.* 2011).

In the self-contamination scenario, the star needs to pass through the AGB phase of evolution in order to undergo s-process nucleosynthesis. However, the evolutionary stage of CEMP-r/s stars studied so far reveals that they have not yet passed through the Red Giant Branch phase to produce the s-process elements. For this reason, this scenario had been rejected by many au-

thors (Jonsell *et al.* 2006, Abate *et al.* 2016). Two objects CS 29503–010 and CS 29528–028 in our sample, exhibit  $\log g$  values ( $\sim 4.0$ ), similar to that of dwarfs or sub-giants. The rest of the stars show low values ( $\sim 1 - 24$ ) of  $^{12}\text{C}/^{13}\text{C}$  implying the extrinsic nature of heavy-elements and carbon in these stars. Thus, this scenario is not applicable to our sample stars.

In another scenario, the primary, being more massive than the other in the binary system formed from the r-process material enriched ISM, evolves faster and proceeds through the AGB phase producing s-process elements along with carbon. The mass transfer episodes in the AGB phase then make the secondary star enriched in s-process elements. Considering this scenario of pre-enrichment of the binary system with r-process elements from the r-rich molecular cloud, Bisterzo *et al.* (2011, (2012) tried to reproduce the observed [hs/lr] in the CEMP-r/s stars. Although they claimed to be successful in doing so (compatible within error bars), there are still some arguments against this scenario. It is found that the abundances of Ba and Eu correlate in CEMP-r/s stars and the AGB models cannot explain this correlation in case of independent enrichment of s- and r-process elements (Abate *et al.* 2016). Also, the large fraction of CEMP-r/s stars among the CEMP-s stars cannot be explained by this scenario (Jonsell *et al.* 2006; Lugaro *et al.* 2009).

(iii) This scenario explains how a star can acquire s- and r-process elements in a triple star system. The

most massive one, among the three stars, evolves the fastest and supernova explosion of this star makes the other two stars r-rich. Then, the more massive one among the other two stars evolves through the AGB phase and produces s-process elements along with carbon. AGB Mass-transfer from this star makes the tertiary a CEMP-r/s star (Cohen *et al.* 2003; Jonsell *et al.* 2006). However, it seems very unlikely that after the SN explosion the triple system survives for further mass transfer. Abate *et al.* (2016) couldn't reproduce the observed frequency of CEMP-r/s stars among CEMP-s stars and hence dismissed this scenario.

(iv) There are two proposed scenarios that considered binary systems where the s-process elements in the CEMP-r/s star are assumed to come from the primary through its AGB phase and r-process elements are attributed to either Type 1.5 supernova (Jonsell *et al.* 2006; Zijlstra 2004) or an accretion-induced collapse (AIC) (Qian & Wasserburg 2003; Cohen *et al.* 2003).

In the first scenario, the primary star, being more massive than the other in the binary system, evolves through the AGB phase. During the AGB phase, the star produces and transfers s-process rich material to the companion. Then, the AGB star may explode as a Type 1.5 supernova and pollute the companion with r-process elements making the secondary a CEMP-r/s star. Iben & Renzini (1983) gave the name 'Type 1.5 supernovae' to the process when the degenerate cores of high mass AGB stars, due to low mass-loss efficiency at low-metallicity, remain as massive as to reach Chandrasekhar mass limit and explode (Zijlstra 2004). However, Nomoto *et al.* (1976), Iben & Renzini (1983) and Lau *et al.* (2008) stated that Type 1.5 supernova can destroy the primary star and hence disrupt the binary system. As most of the CEMP-r/s stars are reported to be found in binary systems (Lucatello *et al.* 2005) Abate *et al.* (2016) rejected this scenario.

In the other scenario, after transferring the AGB processed material (s-process elements) to the companion star, the primary star becomes a white dwarf. Then, as time progresses the secondary star evolves to giant branch and transfers material back to the white-dwarf. This mass-transfer may trigger an accretion-induced collapse (AIC) and hence pollute the secondary star with r-process material (Qian & Wasserburg 2003; Cohen *et al.* 2003). This scenario demands the secondary star to be in the giant branch to fill the Roche-lobe for the second phase of mass-transfer. This scenario may be rejected as the observed CEMP-r/s stars are not always giants (Lugaro *et al.* (2009)). In many cases, these stars are seen in the main-sequence turn-off making the accretion process difficult. Abate *et al.* (2016) stated that the three phases of mass-transfer work properly only if the orbital separation of the binary system is

narrow, but, the observed frequency of CEMP-r/s stars could not be reproduced even by considering a narrow separation. Also, there are uncertainties regarding the efficiency of AIC to produce enough r-process elements to match the observed abundances of heavy-elements in CEMP-r/s stars (Qian & Woosley 1996; Qian & Wasserburg 2003).

(v) A formation scenario named "intermediate neutron-capture process or i-process", similar to that of the formation scenarios of CH, Ba and CEMP-s stars has been proposed recently to explain the abundances of CEMP-r/s stars. This scenario considers a binary system, where one star is slightly massive than the other. The more massive star evolves faster and passes through the AGB phase polluting the companion with AGB processed material. The difference of this scenario with that of the s-process enrichment scenarios is that in this scenario a neutron density ( $n \sim 10^{15} \text{ cm}^{-3}$ ), which is intermediate to the neutron-densities of both s- and r-process, can produce the double enhancement seen in CEMP-r/s stars (Cowan & Rose 1977; Dardélet *et al.* 2014; Hampel *et al.* 2016). Cowan & Rose (1977), for the first-time, suggested the possibility of occurrence of i-process in AGB stars. They found that significantly high neutron-density can be achieved by mixing hydrogen-rich material into the intershell region of AGB stars. Using i-process models Dardélet *et al.* (2014) and Hampel *et al.* (2016) have successfully reproduced the abundance distribution of a number of well-known CEMP-r/s stars.

#### 4.2 Comparison of the abundance pattern of the sample stars with i-process model

Dardélet *et al.* (2014) and Hampel *et al.* (2016) calculated i-process model yields with slightly different approaches, but, both the groups could successfully reproduce the observed abundance pattern of CEMP-r/s stars. Single-zone nuclear network calculations were used in both the studies. Assuming proton-ingestion from the H-rich envelope to the He pulse-driven convective zone (PDCZ) to be responsible for the generation of higher neutron-densities ( $n \sim 10^{15} \text{ cm}^{-3}$ ) Dardélet *et al.* (2014) used a constant combined mass-fraction of C+H (= 0.7) in their simulations. They considered the termination time of the i-process as a free parameter for their calculations. On the other hand, Hampel *et al.* (2016) calculated the yields of the neutron-capture nucleosynthesis, assuming the nucleosynthesis to operate in the intershell region of an AGB star, at different constant neutron-densities starting from  $n \sim 10^7 \text{ cm}^{-3}$  to  $10^{15} \text{ cm}^{-3}$ . Dardélet *et al.* (2014) assumed the temperature and density for the He PDCZ to be  $2.0 \times 10^8 \text{ K}$  and  $10^4 \text{ g cm}^{-3}$  respectively. These physical input parameters are chosen so as to

prevent the proton capture by  $^{13}\text{N}$  and allow the  $^{13}\text{C}(\alpha, n)^{16}\text{O}$  reaction for neutron-release. As a test, Hampel *et al.* (2016) tried to calculate the yields with a range of temperatures ( $1 \times 10^8$  K to  $2.2 \times 10^8$  K) and densities ( $800 \text{ gcm}^{-3}$  to  $3200 \text{ gcm}^{-3}$ ), but, didn't see significant changes in the results. However, for the final simulations they adapted the parameters ( $T = 1.5 \times 10^8$  K and  $\rho = 1600 \text{ gcm}^{-3}$ ) of the intershell region of a low-metallicity ( $z = 10^{-4}$ ), low-mass ( $M = 1 M_{\odot}$ ) AGB star (Stancliffe *et al.* 2011). As initial abundances of the He PDCZ, Dardelet *et al.* (2014) considered solar-abundances (except C and O), scaled down to  $z = 10^{-3}$ . The abundances of C and O are taken to be  $X(^{12}\text{C})=0.5$  and  $X(^{16}\text{O})=0.05$ , which are typical abundances for the He PDCZ. Whereas Hampel *et al.* (2016) adapted the constituents of the intershell region from that of Abate *et al.* (2015). A high neutron exposure of  $\tau \sim 495 \text{ mb}^{-1}$  is ensured by adjusting the run times of the models. Due to such high neutron exposures, the abundance pattern of heavy elements and the seed nuclei comes to an equilibrium, which makes the element-to-element ratio a function of constant neutron-density.

In the model of Dardelet *et al.* (2014), almost all the isotopes of  $^{12}\text{C}$  get transformed into  $^{13}\text{N}$  during the first second of run-time. Then in 9.97 minutes,  $^{13}\text{N}$  decays to form  $^{13}\text{C}$ , which captures  $\alpha$  to release neutrons with high neutron-densities through the reaction  $^{13}\text{C}(\alpha, n)^{16}\text{O}$ . The neutron-exposure ( $\tau$ ) increases with time reaching up to  $10 - 50 \text{ mb}^{-1}$  and subsequently the heavier elements are produced. This model could successfully reproduce the observed abundance pattern of three CEMP-r/s stars. On the other hand, Hampel *et al.* (2016) noticed that when the neutron exposure was kept switched on, for lower neutron densities ( $n \sim 10^7 \text{ cm}^{-3}$ ), typical s-process abundance pattern is produced with stable peaks of ls (Sr, Y, Zr) and hs (Ba, La, Ce) elements. But with higher neutron-densities ( $n = 10^{12} - 10^{15} \text{ cm}^{-3}$ ), both the peaks of ls and hs elements shift to lighter elements. In particular, a peak at  $^{135}\text{I}$  is formed due to the i-process neutron-densities. Then, the neutron exposure is turned off for  $t = 10 \text{ Myr}$ . During this time, it is noticed that unstable isotopes decay to produce stable isotopes at ls and hs peaks. The decay of  $^{135}\text{I}$  produces  $^{135}\text{Ba}$ . With increasing neutron-densities abundances of Ba and Eu are found to increase. This is how the abundance pattern gets modified due to i-process. Using this i-process model, Hampel *et al.* (2016) could successfully reproduce the observed abundance pattern of twenty CEMP-r/s stars, including the three previously reproduced by the i-process model of Dardelet *et al.* (2014).

We have used the model predictions ( $[\text{X}/\text{Fe}]$ ) for neutron densities ranging from  $n \sim 10^9 - 10^{15} \text{ cm}^{-3}$  (Hampel *et al.* (2016)), and compared with the elemen-

**Table 4. Fit parameters of i-process model for the sample stars**

Star name	Neutron-density $n \text{ (cm}^{-3}\text{)}$	d	$\chi^2$
CD-28 1082	$10^{13}$	0.9704	3.26
CS 29503-010	$10^{13}$	0.9745	2.74
CS 29528-028	$10^{12}$	0.9331	0.51
HD 209621	$10^{13}$	0.9798	3.52
HE 0002-1037	$10^{14}$	0.9766	1.71
HE 0059-6540	$10^{13}$	0.9908	2.34
HE 0151-6007	$10^{14}$	0.9274	2.06
HE 1305+0007	$10^{14}$	0.9262	2.62

tal abundance pattern of our sample of CEMP-r/s stars. In order to examine whether the i-process models could reproduce the observed abundances of the sample stars we have followed the procedure discussed in Hampel *et al.* (2016) and used the equation-

$$X = X_i \times (1 - d) + X_{\odot} \times d \quad (1)$$

where  $X_i$  is the model yield,  $X_{\odot}$  is solar-scaled abundance and  $d$  is a dilution factor.

Table 4 presents the values of the fit parameters neutron-density, 'd' and ' $\chi^2$ ' for each star. The best fit neutron-density for each of the sample stars is chosen for which we got the minimum value of ' $\chi^2$ '. The best fit models with appropriate neutron-densities and corresponding dilution factors are shown in Figure 2. We have found that i-process models with neutron-densities of  $n \sim 10^{12} \text{ cm}^{-3}$  to  $10^{14} \text{ cm}^{-3}$  closely fit the observed abundances of the sample stars. We have obtained a neutron-density of  $n \sim 10^{14} \text{ cm}^{-3}$  for the star HE 1305+0007, which is same as reported by Hampel *et al.* (2016) for the object. Hampel *et al.* (2019) tried to understand the i-process nucleosynthesis through the abundances of Pb in the CEMP-r/s stars. In their i-process models Hampel *et al.* (2019) considered neutron-exposure ( $\tau$ ) as a free parameter along with dilution factor (d). Varying 'd' and ' $\tau$ ' at different constant neutron-densities, they could fit the observed abundances of HE 1305+0007 and HD 209621 with models of neutron-densities,  $n \sim 10^{14} \text{ cm}^{-3}$  and  $10^{13} \text{ cm}^{-3}$  respectively. We, too, got the best fit at  $n \sim 10^{13} \text{ cm}^{-3}$  for the object HD 209621 taking only 'd' as a free parameter with constant ' $\tau$ '.

## 5. Conclusions

In this study, we have examined if the currently available theoretical i-process stellar yields could adequately explain the enhancement in both s- and r-process elements observed in a selected sample of

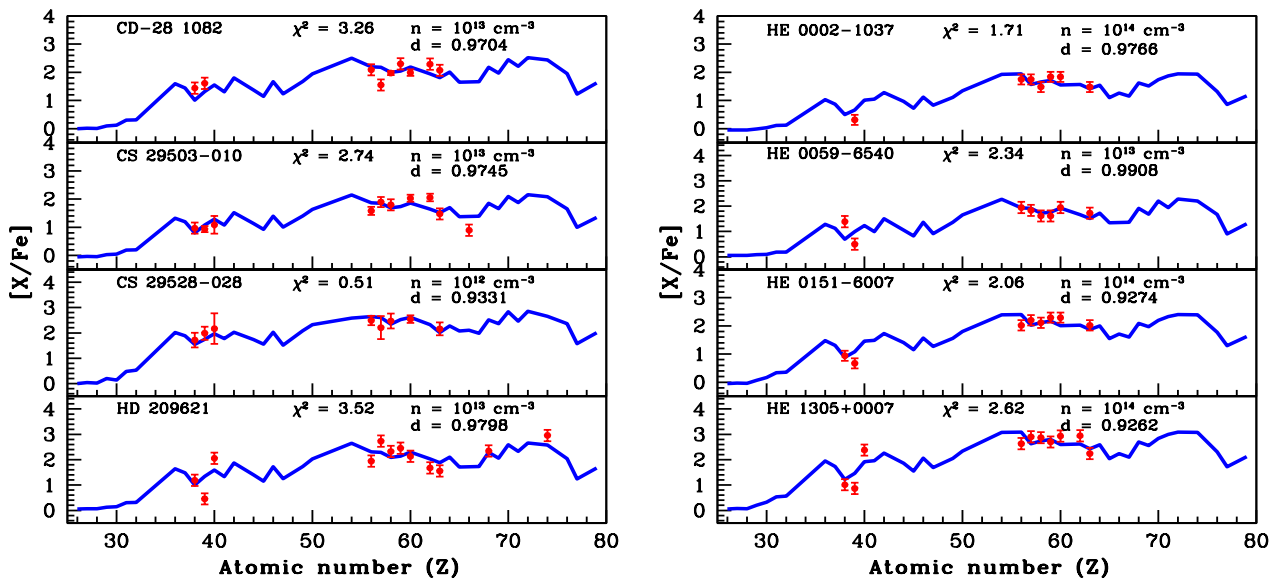


**Figure 2.** Best-fitting i-process model (solid blue curve) for the sample stars. The points with error bars indicate the observed abundances.

CEMP-r/s stars. We have considered eight stars, out of which, the abundances of the heavy elements for three objects are taken from our previous studies (Goswami et al. 2006, Goswami & Aoki 2010, Purandardas et al. 2019) and the rest from other sources (Allen et al. 2012, Hansen et al. 2019).

With the help of a parametric-model based study, we have estimated the contributions from s- and r-process nucleosynthesis to the observed elemental abundances. It is found that similar contributions from both the processes are required to explain the observed abundance pattern of heavy-elements in these stars.

With reference to the double enhancement seen in the sample stars, we have discussed different formation scenarios of CEMP-r/s stars. The scenarios involving two stellar sites for the production of s- and r-process elements are found to be not applicable to the sample of CEMP-r/s stars under this study. However, we have seen that i-process models of Hampel *et al.* (2016) can satisfactorily reproduce the observed overabundance of heavy elements in these stars. The i-process stellar yields required to fit the observed abundance patterns are found to correspond to neutron-densities as high as  $10^{12} \text{ cm}^{-3}$  to  $10^{14} \text{ cm}^{-3}$ . The estimated low values of  $^{12}\text{C}/^{13}\text{C}$  ratio observed in the stars agree well with the i-process predictions indicating the extrinsic nature of carbon and the heavy elements.

## Acknowledgements

The funding from the DST SERB project EMR/2016/005283 is gratefully acknowledged. We are thankful to Melanie Hampel for providing us with the i-process yields in the form of number fractions. This work made use of the SIMBAD astronomical database, operated at CDS, Strasbourg, France and the NASA ADS, USA.

## References

- Abate, C., Pols, O. R., Karakas, A. I., & Izzard, R. G. 2015, *A&A*, 576, A118
- Abate, C., Stancliffe, R. J., & Liu, Z.-W. 2016, *A&A*, 587, A50
- Allen D. M., Ryan S. G., Rossi S., Beers T. C., Tsangarides S. A., 2012, *A&A*, 548, A34
- Aoki, M, Ishimaru, Y., Aoki, W., Wanajo, S., 2017, *ApJ*, 837, 8
- Aoki, W., Beers, T. C., Christlieb, N., Norris, J. E., Ryan, S. G. & Tsangarides, S. 2007, *ApJ* 655, 492.
- Aoki, W., Suda T., Beers, T. C., Honda, S., 2015, *AJ*, 149, 39
- Arlandini, C., Käppeler, F., Wisshak, K., et al. 1999, *ApJ*, 525, 886
- Beers, T. C. & Christlieb, N. 2005, *ARA&A*, 43, 531
- Bisterzo, S., Gallino, R., Straniero, O., Cristallo, S., & Kappler, F. 2011, *MNRAS*, 418, 284

- Bisterzo, S., Gallino, R., Straniero, O., Cristallo, S., & Kappeler, F. 2012, *MNRAS*, 422, 849
- Busso, M., Gallino, R., & Wasserburg, G. J. 1999, *ARA&A*, 37, 239
- Cohen, J. G., Christlieb, N., Qian, Y.-Z., & Wasserburg, G. J. 2003, *ApJ*, 588, 1082
- Cowan, J. J. & Rose, W. K. 1977, *ApJ*, 212, 149
- Dardelet, L., Ritter, C., Prado, P., et al. 2014, in *Proc. XIII Nuclei in the Cosmos Symp.*, ed. Z. Elekes & Z. Fülöp (Trieste: PoS), 145
- Doherty, C. L., Gil-Pons, P., Siess, L., Lattanzio, J. C., & Lau, H. H. B. 2015, *MNRAS*, 446, 2599
- Fujimoto, M. Y., Iben, Jr., I., & Hollowell, D. 1990, *ApJ*, 349, 580
- Gallino R., Arlandini C., Busso M., Lugaro M., Travaglio C., Straniero O., Chieffi A., Limongi M., 1998, *ApJ*, 497, 388
- Goswami, A., & Aoki, W. 2010, *MNRAS*, 404, 253
- Goswami, A., Aoki, W., Beers, T. C., et al. 2006, *MNRAS*, 372, 343
- Goswami, A., Athiray, S. P., & Karinkuzhi, D. 2010, *Astrophysics and Space Science Proceedings*, 17, 211
- Hempel, M., Karakas, A. I., Stancliffe, R. J., Meyer, B. S., & Lugaro, M. 2019, *ApJ*, 887, 11
- Hempel, M., Stancliffe, R. J., Lugaro, M., & Meyer, B. S. 2016, *ApJ*, 831, 171
- Hansen, C. J., Hansen, T. T., Koch, A., et al. 2019, *A&A*, 623, A128
- Hill, V., Barbuy, B., Spite, M., et al. 2000, *A&A*, 353, 557
- Iben, Jr., I. & Renzini, A. 1983, *ARA&A*, 21, 271
- Ivans I. I., Sneden C., Gallino R., Cowan J. J., Preston G. W., 2005, *ApJ*, 627, L145
- Jones, S., Ritter, C., Herwig, F., et al. 2016, *MNRAS*, 455, 3848
- Jonsell, K., Barklem, P. S., Gustafsson, B., et al. 2006, *A&A*, 451, 651
- Lau, H. H. B., Stancliffe, R. J., & Tout, C. A. 2008, *MNRAS*, 385, 301
- Lucatello, S., Gratton, R. G., Beers, T. C., & Carretta, E. 2005, *ApJ*, 625, 833
- Lugaro, M., Campbell, S. W., & de Mink, S. E. 2009, *PASA*, 26, 322
- Matrozi, E. & Stancliffe, R. J. 2016, *A&A*, 592, A29
- Nomoto, K., Sugimoto, D., & Neo, S. 1976, *Ap&SS*, 39, L37
- Purandardas, M., Goswami, A., Goswami, P. P., Shejeelamal, J., & Masseron, T. 2019, *MNRAS*, 486, 3266
- Qian, Y. Z. & Wasserburg, G. J. 2003, *ApJ*, 588, 1099
- Qian, Y. Z. & Woosley, S. E. 1996, *ApJ*, 471, 331
- Richard, O., Michaud, G., Richer, J., et al. 2002, *ApJ*, 568, 979
- Stancliffe, R. J., Dearborn, D. S. P., Lattanzio, J. C., Heap, S. A., & Campbell, S. W. 2011, *ApJ*, 742, 121
- Thielemann, F.-K., Arcones, A., Kappeli, R., et al. 2011, *PrPNP*, 66, 346
- Tsuji T., Tomioka K., Sato H., Iye M., Okada T., 1991, *A&A*, 252, L1
- Wehmeyer, B., Pignatari, M., & Thielemann, F.-K. 2015, *MNRAS*, 452, 1970
- Zijlstra, A. A. 2004, *MNRAS*, 348, L23